Supporting information

Identification of phosphate-containing compounds as new inhibitors of 14-3-3/c-Abl protein-protein interaction

Leire Iralde-Lorente, Giusy Tassone, Letizia Clementi, Lorenzo Franci, Claire C Munier, Ylenia Cau, Mattia Mori, Mario Chiariello, Adriano Angelucci, Matthew W.D. Perry, Cecilia Pozzi, Stefano Mangani, Maurizio Botta.

Table of content

Results SI-1. Crystal structures of ligand-free h14-3-3σ and its complexes with IMP and PLP S3
Results SI-2. Validation of the h14-3-3/c-Abl peptide interaction S3

Method SI-1. Expression and purification h14-3-3 proteins S4
Method SI-2. Protein crystallography S6
Method SI-3. Synthesis of FITC labelled c-Abl peptide S8
Method SI-4. FP competitive assays S8
Method SI-5. Selection of molecules S9
Method SI-6. Synthetic procedures S10
Method SI-7. Viability Assay on K-562 and HS27 cells S11
Method SI-8. Cells, cell culture, and transfections S12
Method SI-9. Immunofluorescence, confocal microscopy, and densiometric analysis S12
Figure SI-1 S14
Figure SI-2. S14
Figure SI-3. S15
Figure SI-4. S16
Figure SI-5. S16

Figure SI-6. S17
Figure SI-7. S17
Table SI-1. S18
Table SI-2. S19
Abbreviation list S20
References S21

Results SI-1. Crystal structures of ligand-free h14-3-3σ and its complexes with IMP and PLP

The structure of h14-3-3σ and its complexes with IMP and PLP were obtained at resolution ranging from 2.40 Å to 3.00 Å. The protein chain was completely rebuilt apart from the last 17 C-terminal residues. On the other hand, in the N-terminal region of all structures a five amino acid extension was modelled due to the His^6-tag cleavage (including all residues starting from the cleavage site, Figure SI-1). Two highly flexible regions, consisting of residues 71-77 and 206-214, are present in all structures. The poor quality of the electron density in these regions prevented us from rebuilding them in our models. Further, an additional flexible loop, including residues 108-112 was not modelled in chain B of the complex with PLP. In all structures, the presence of sulfate ions arising from the crystallization conditions was detected inside the amphipathic groove or in various sites on the solvent-exposed protein surface. The binding in the amphipathic groove of the sulfate ion in the ligand-free h14-3-3σ and of IMP and PLP in the respective complexes, was validated during PDB depositions by the calculation of the real space correlation coefficients (RSCC). RSCC values higher than 0.80 were obtained for the sulfate ion and the ligands, indicating a good fit in all models (Table SI-1).

Results SI-2. Validation of the h14-3-3/c-Abl peptide interaction

Earlier studies on the c-Abl/h14-3-3 (σ and ζ isoforms) interaction have shown that the recognition within the h14-3-3 amphipathic groove depends on the phosphorylation of the c-Abl Thr735, belonging to the conserved motif $RSVT^{735}LP$.[1] On this basis, we have synthesized an 11-mer peptide (EWRSVT^{p}LPRDL) including a phospho-threonine (T^p) in position 6 and covering the c-Abl protein segment 730-740. The peptide was then N-

terminally labelled with the fluorescent dye fluorescein isothiocyanate (FITC). The binding properties of the resulting fluorescent-labelled peptide to h14-3-3σ and h14-3-3ζ were investigated by FP and SPR analysis. K_d values of 48 μM and 30 μM, were determined for the σ and ζ isoform, respectively, through FP-based direct assays (Figure SI-2A). The h14-3-3/c-Abl interaction was further confirmed by SPR analysis giving K_d values of 30 μM for the σ isoform and of 8.9 μM for h14-3-3ζ (Figure SI-2B). The SPR data showed reduced standard deviation with respect to those obtained by FP analysis. The reduced K_d values characterized by SPR analysis could be attributed to the higher sensitivity and accuracy of the SPR technique that provides better quality data. Despite these fluctuations in the K_d values, both assays converged in reporting more effective binding of the c-Abl peptide to the h14-3-3ζ isoform.

Even though various phospho-peptides have been investigated for their binding to h14-3-3 proteins, no peptides including the motif RSVT^{p}LP (or analogous sequences), have been described previously. Nonetheless, K_d values comparable to those determined for our c-Abl peptide have been reported for slightly longer phospho-serine peptides through FP analysis.[2]

Method SI-1. Expression and purification of h14-3-3 proteins

The vector plasmid pPROEX-HTb – h14-3-3σ (including the gene coding sequence for h14-3-3σ, cloned within the BamHI – NotI restriction sites, and a TEV-cleavable His^{6}-tag) was a kind gift of Professor Christian Ottmann (Department of Biomedical Engineering, Eindhoven University of Technology, Netherlands). Recombinant h14-3-3σ was prepared as previously described,[3] with minor modifications. Briefly, the protein was

expressed in the *Escherichia coli* strain BL21(DE3) and purified by nickel affinity chromatography (HisTrap FF 5 mL column, GE Healthcare) in a three step gradient. The target protein was eluted applying a 500 mM imidazole concentration in buffer A (250 mM NaCl and 50 mM Tris-HCl, pH 8). Fractions containing the target protein were pooled and dialyzed in buffer A at 4 °C. The resulting protein sample was divided into two pools. Pool A, containing the His^6-h14-3-3σ, was used for biophysical assays. Pool B, used for structural studies, was subjected to His^6-tag removal by incubating the target protein with 0.05 mg of in house produced His^6-tag TEV protease (HT-TEV)[4] at 4 °C. After 24 h tag cleavage was complete (> 98 %, as verified by SDS-PAGE analysis), thus the mature protein (h14-3-3σ, having an N-terminal extension of 5 amino acids due to the TEV proteolytic cleavage, Figure SI-1) was separated from the residual His^6-h14-3-3σ and the HT-TEV by a second nickel affinity chromatography. The His^6-tag cleavage was also confirmed by dot blot analysis using an HRP-conjugated monoclonal antibody specifically recognizing exa-histidine sequences on target proteins (His^6-tag Ab, Thermo Fisher). The high purity (> 98 %) of h14-3-3σ was confirmed by SDS-PAGE analysis and MALDI-TOF mass spectrometry. The final yield was estimated to 72-87 mg of target protein per liter of bacterial culture.

Human 14-3-3ζ was cloned in the pET104.1 DEST vector as His^6-linker (MSYYHHHHHHDYDIPTTENLYFQGAMGS) – h14-3-3ζ and expressed in the *E. coli* BL21(DE3)STAR strain. Bacteria were cultured in the TB medium supplemented with 3 mM $MgCl_2$, 0.02 % v/v glucose, 0.8 % v/v glycerol and 50 μg mL^{-1} carbenicillin at 37 °C to an OD_{600} of 0.4-0.6. The overexpression of the target protein was induced overnight at 18 °C by adding 0.4 mM IPTG. Cells were harvested by centrifugation (5000g, 20 min), resuspended in lysis buffer (50 mM Tris, 300 mM NaCl, 12.5 mM imidazole, 1 mM TCEP,

and 5 mM $MgCl_2$, supplemented with the Roche protease inhibitor) and lysed using a cell disruptor (Constant Systems LTD) at 25 ksi. After centrifugation (35000g, 45 min), the lysate was incubated overnight at 4 °C with the Ni-NTA Agarose resin (Qiagen). The nickel-resin was then washed with the lysis buffer added by 0.1 % v/v Triton X-100 and h14-3-3ζ eluted using a 250 mM imidazole concentration. The target protein was further purified by size exclusion chromatography on an HiLoad 26/60 Superdex75pg (Pharmacia Biotech) column equilibrated with HBS P+ buffer. Fractions containing h14-3-3ζ were combined and concentrated to 87 mg mL^{-1} and the aliquots frozen in liquid nitrogen and stored at -80 °C (until required).

Method SI-2. Protein crystallography

Before crystallization experiments, h14-3-3σ was concentrated to 20 mg mL^{-1} in buffer B (500 mM NaCl and 50 mM sodium citrate, pH 5.0). Crystallization of h14-3-3σ was performed as described by Benzinger *et al,*[5] with minor modifications. Briefly, crystals of h14-3-3σ were grown using the hanging drop vapor diffusion method[6] by mixing equal volumes of protein (added by 5 mM dithiothreitol) and precipitant (40 % wt/vol PEG-4000, 600 mM ammonium sulfate and 100 mM Tris-HCl, pH 9.0) solutions, equilibrated over a 600 µL reservoir at 8 °C. Crystals, appeared after few days, were washed in the cryo-protectant solution, prepared by adding 20% v/v PEG-400 to the precipitant solution and flash frozen in liquid nitrogen. Crystals of h14-3-3σ were used to perform an X-ray crystallographic screening using the series 1 compounds. In the screening, preformed protein crystals were soaked for 3 hours with 5 mM of each compound

added directly in the crystallization drop (0.4 µL of 50 mM compound solution added to ~ 4 µL crystallization drop).

X-ray diffraction images were collected at 100 K using synchrotron radiation at the Diamond Light Source (DLS, Didcot, UK) beamline I04 equipped with a Pilatus 6M-F detector and at the European Synchrotron Radiation Facility (ESRF, Grenoble, France) beamline ID30-B, on a Dectris Pilatus3 6M detector. Data were integrated using either Mosflm 7.2.1[7] or XDS[8] and scaled with SCALA[9,10] from the CCP4 package.[11] Molecular replacement was performed with the program Molrep[12] using the structure of h14-3-3σ (PDB id 1YZ5)[13] as the searching model (excluding non-protein atoms and water molecules). The analysis of the solvent content indicated the presence of two protein molecules in the ASU of both crystals of ligand-free h14-3-3σ and of the IMP complex (Matthews coefficient[14] of 2.2 and 2.4, respectively), and of four molecules in the ASU of the PLP complex (Matthews coefficient of 2.4). However, molecular replacement provided solutions only with one (ligand-free and IMP complex) and two protein chains (PLP complex), corresponding to an estimated solvent content of ~ 73%. The models were refined by using the program REFMAC5[15] of the CCP4 package. The molecular graphic software Coot[15] was used for manual rebuilding and modelling of missing atoms and to add solvent molecules. Upon completion of the ligand-free h14-3-3σ model, inspection of the Fourier difference map, clearly demonstrated the presence of five sulfate anions and one di(hydroxyethyl)ether molecule. On the other hand, two sulfate anions and a PLP molecule were added in the h14-3-3σ – PLP complex and a sulfate anion and an IMP molecule in the h14-3-3σ – IMP complex. Final models were inspected manually and checked with the programs Coot and Procheck.[15,16] All models were completely rebuilt apart for the last 17 C-terminal residues. Data collection and

refinement statistics are summarized in Table SI-1. Figures were generated using Pymol.[17] Coordinates and structure factors were deposited in the PDB under the codes 6TLG (h14-3-3σ), 6TM7 (h14-3-3σ – PLP), and 6TLF (h14-3-3σ – IMP).

Method SI-3. Synthesis of FITC labelled c-Abl peptide

The peptide EWRSVT^{p}LPRDL was synthesized on a chlorotrityl resin (303 mg, 0.66 mmol/g loading) via Fmoc solid-phase peptide synthesis (SPPS) using a Biotage Alstra automated peptide synthesizer. Side-chain protection was performed by using Bzl for pThr, t-Bu for Glu and Ser, Pbf for Arg and Boc for Trp. FITC label was added manually on the N-terminal of the peptide conjugated by an aminocaproic acid linker (Fmoc-6-Ahx-OH) under the standard SPPS conditions. Final deprotection and cleavage were achieved by treatment with a mixture of TFA/TIS/H_2O (95:2,5:2,5, v/v/v) at room temperature (rt). The reaction mixture was shaken for 3 h at rt. TFA solution was then collected and the resin was rinsed three times with 1 mL TFA. The peptide was precipitated with a cold solution of diethyl ether, centrifuged and lyophilised. The peptide was purified by preparative reversed-phase HPLC (column Waters Acquity CSH C18 1.7 μm) coupled with MS detection (Figure SI-4).

Method SI-4. FP competitive assays

The percentage of maximum inhibition was calculated by the following equation:

$$Max.\,\%\,inhibition = \frac{mP_N - mP_S}{mP_N - mP_P} \cdot 100$$

Where, mP_N and mP_P represent the FP signal value of the negative control (FP signal of solution **A**) and the positive control (FP signal of solution **B**), respectively. mP_S represents the FP signal value of each small molecule (FP signal of the solution **D**).

Dose-response curves provided the IC_{50} values (Figure SI-6 and SI-7). To facilitate the direct comparison of the inhibitory activity, IC_{50} values were used to calculate the absolute inhibition constant (K_i) through the Cheng-Prusoff equation: [18]

$$Ki = \frac{IC_{50}}{\frac{[L]}{Kd} + 1}$$

Where:

[L] is the concentration of the labelled peptide; K_d is the dissociation constant; IC_{50} is the compound concentration required to displace 50% of the peptide-protein binding. Since the concentration (60 nM) of the labelled peptide used in the assays is low, the variation between the IC_{50} and the K_i is negligible.

Method SI-5. Selection of Molecules

Molecules of the A and B series were selected and purchased from commercially available libraries from MolPort (https://www.molport.com) and Aldrich Market Select (https://www.aldrichmarketselect.com) (Table SI-2). Molecules were selected according to their structural analogy to either PLP or IMP, using a similarity index threshold of 0.8.

Compounds of the C series included phospho-derivatives were chosen to study the effect of the phosphate group on the molecule binding. The D series was selected according to the results of the FP screening performed on the compounds of the A and

B series. A further series was added for the present study, the E series, designed to include *meta*- and *para*- derivatives of PLP. Four compounds of the C, D, and E series were synthesized according to the procedures described below.

Method SI-6. Synthetic procedures

Benzylphosphonic acid (C1S)

To a solution of Diethyl benzylphosphonate (100 mg, 0,44 mmol, 1 eq) in 10 mL of DCM, bromotrimethylsilane (0.613 mL, 5.26 mmol, 12 eq) was added. The mixture was stirred at rt for 24h. Then, the solvent was removed. The solid was dissolved in 10 mL of MeOH. The mixture was stirred at rt for 2h. Then, the solvent was removed under vacuum and H_2O and DCM were added to the residue. The aqueous phase was recovered and evaporated to give a white solid. Yield: 99% (75 mg, 0.436 mmol). ^{1}H NMR (500 MHz, DMSO, 298K) (ppm): δ= 7.25 (m, 5H); 2.94 (d, J = 20 Hz, 2H).

(2-oxo-2-phenylethyl)phosphonic acid (C6S)

Compound C6S was synthesized starting from diethyl(2-oxo-2-phenylethyl)phosphonate (100 mg, 0,39 mmol, 1 eq) following procedure indicated for compound C1S. Yield: 96 % (75 mg, 0.37 mmol). ^{1}H NMR (500 MHz, DMSO, 298K) (ppm): δ= 8.01 (d, J = 7.7 Hz, 2H); 7.63 (t, J = 7.3 Hz, 1H); 7.52 (t, J = 7.6 Hz, 2H); 3.52 (d, J = 20 Hz, 2H).

(2-(benzyloxy)-2-oxoethyl)phosphonic acid (C7S)

Compound C7S was synthesized starting from Benzyl 2-(dimethoxyphosphoryl)acetate (100 mg, 0,39 mmol, 1 eq) following procedure indicated in compound C1S. Yield: 96 %

(74.9 mg, 0.37 mmol). ^{1}H NMR (500 MHz, DMSO, 298K) (ppm): δ= 7.33 (m, 5H); 5.23 (s, 2H); 2.94 (d, J = 20 Hz, 2H).

(5-Hydroxy-6-methyl-4-((phenylamino)methyl)pyridin-3-yl)methyl dihydrogen phosphate (E2S)

4-Formyl-5-hydroxy-6-methylpyridin-3-yl)methyl dihydrogen phosphate (100 mg, 0.40 mmol, 1 eq) and aniline (37 µL, 0.40 mmol, 1 eq) were mixed in DCE (4 mL) and stirred at rt. Sodium triacetoxyborohydride (120 mg, 0.57 mmol, 1.4 eq) and AcOH (23 µL, 0.40 mmol, 1 eq) were added to the mixture. The mixture was stirred at rt under N_2 atmosphere for 24 hours. Solvents were removed in the rotavaport. The resulting oil was treated with NaOH 1M and DCM. The aqueous layer was separated and lyophilised to give an orange solid. Yield**:** 88 % (114 mg, 0.352 mmol). ^{1}H NMR (500 MHz, $CDCl_3$, 298K) (ppm): δ= 7.38 (s, 1H); 7.10 (t, J = 7.8 Hz, 2H); 6.79 (d, J = 7.9 Hz, 2H); 6.67 (t, J = 7.4 Hz, 1H); 4.19 (s, 2H); 2.16 (s, 3H); 2.14 (d, J = 6.1 Hz, 2H). MS (ESI) m/z: 325.3 $[M+H]^+$.

Method SI-7. Viability Assay on K-562 and HS27 cells

In vitro experiments were carried out using human cell line K-562 (erythroleukemia) and Hs27 (diploid fibroblasts). K-562 cells were cultured in RPMI medium with 10% foetal bovine serum (FBS). Hs27 cells were cultured in DMEM medium with 10% FBS. In order to determine the antiproliferative effect of compounds, cells were seeded at density of 5×104 cells/ml (K-562) 5×104 cells/cm^2 and treated with increasing concentrations of selected compounds. Control cells were treated with the vehicle of the experimental point containing the highest percentage of DMSO. Cell cultures were maintained at 37°C in 5% v/v CO_2 for 72 h. Cell number and vitality were evaluated on cell suspension using

the automatic cell counter NucleoCounter® (Chemometec, Denmark). Each experiment was performed at least three times and results were expressed as mean and standard deviation.

Method SI-8. Cells, cell culture, and transfections

HeLa cells stably expressing EGFP-Abl (HeLa EGFP-Abl) were obtained by transfection of HeLa cells with the pCEFL EGFP ABL wild-type expression vector38 using lipofectamine LTX (Life Technologies, Carlsbad, CA), according to the manufacturer's instructions, followed by selection with 2 mg mL^{-1} G418 (SigmaAldrich) for 3 weeks. HeLa EGFP-Abl were maintained in DMEM supplemented with 10% FBS, 2 mM L-glutamine, 10000 UmL^{-1} penicillin, and 10 mg mL^{-1} streptomycin and were constantly kept under selective pressure with 2 mg mL-1 G418. Selective medium was replaced with regular growth medium on the day before experiments.

Method SI-9. Immunofluorescence, confocal microscopy, and densitometric analysis of fluorescence

Cells were washed with PBS, then fixed with 4% paraformaldehyde in PBS for 20 min and permeabilized with 0.1% Triton X-100 in PBS for 30 min. Nuclei were stained with a solution of 6µm of 4',6-diamidino-2- phenylindole (DAPI; Sigma Aldrich) in PBS for 10 min. Coverslips were mounted in fluorescence mounting medium (Dako). Samples were visualized on a TSC SP5 confocal microscope (Leica, 5100000750), installed on an inverted LEICA DMI 6000CS (10741320) microscope and equipped with an oil immersion PlanApo 40x1.25 NA objective. Images were acquired using LAS AF acquisition software

(Leica). Intensitometric analysis of fluorescence was performed using the Quantitation Module of the Volocity software (PerkinElmer Life Science). Briefly, total nuclear EGFP fluorescence, defined as EGFP signal co-staining with DAPI nuclear dye, was measured in six representative confocal fields for each experimental condition. The resulting mean values ±SEM are expressed as a percentage of nuclear EGFP fluorescence. Six representative fields were acquired and analyzed for each sample. Significance (p value) was assessed by t-test. Asterisks were attributed for the following significance values: *****$p<0.0001$.

MSYYHHHHHHDYDIPTTENLYFQ↑GAMGS

MERASLIQKAKLAEQAERYEDMAAFMKGAVEKGEELSCEERNLLSVAYKNVVGGQRAAWRVLSSIEQKSNEEGSEEKGPEV
REYREKVETELQGVCDTVLGLLDSHLIKEAGDAESRVFYLKMKGDYYRYLAEVATGDDKKRIIDSARSAYQEAMDISKKEMPP
TNPIRLGLALNFSVFHYEIANSPEEAISLAKTTFDEAMADLHTLSEDSYKDSTLIMQLLRDNLTLWTADNAGEEGGEAPQEPQS

Figure SI-1. Sequence of His^6-h14-3-3σ. Amino acids belonging to the His^6-tag and to the TEV cleavage site are coloured green and red, respectively. TEV protease catalyses the cleavage of the peptide bond between glutamine and glycine as indicated by the black arrow.

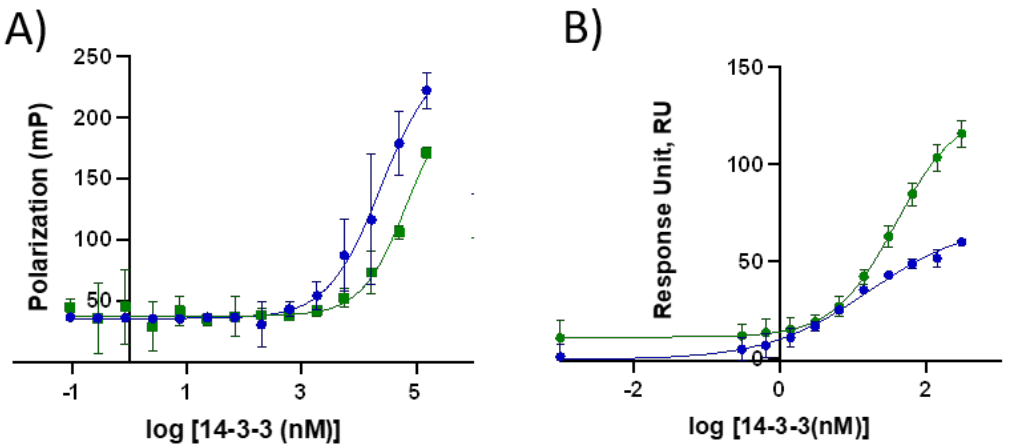

Protein	K_d (μM)
14-3-3ζ	30.0 ± 7.9
14-3-3σ	47.8 ± 2.9

Protein	K_d (μM)
14-3-3ζ	8.9 ± 0.9
14-3-3σ	30.0 ± 0.2

Figure SI-2. Association constants (K_d) of c-Abl peptide binding to 14-3-3σ and 14-3-3ζ. (A) Dose-response curves and affinity constant (K_d) of the FP direct assays. (B) Dose-response curves and K_d values determined by SPR.

Series 1			
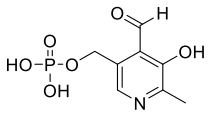	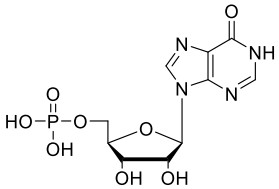	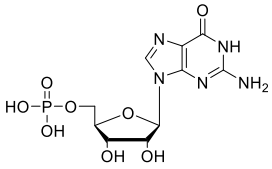	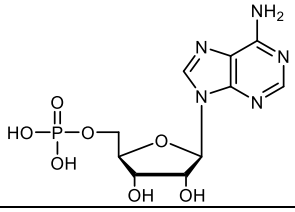
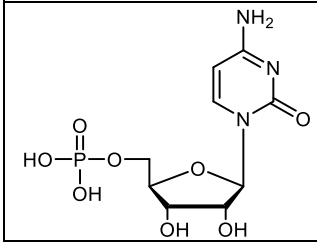	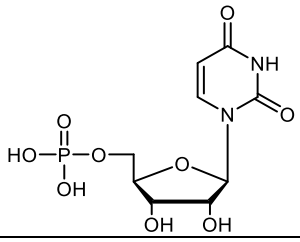		

Figure SI-3. Molecules belonging to the Series 1, including various nucleotides and pyridoxal phosphate (PLP).

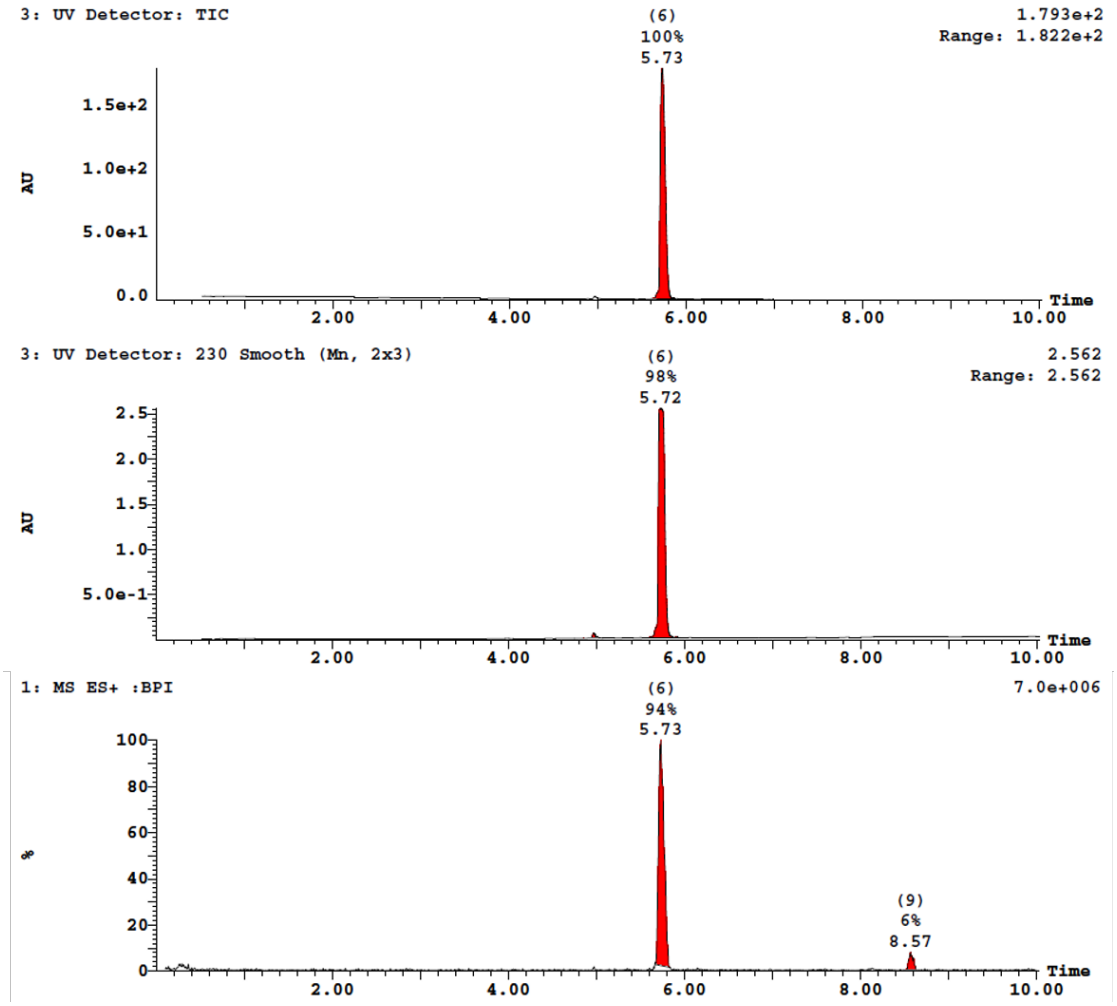

Figure SI-4. LCMS of the c-Abl peptide.

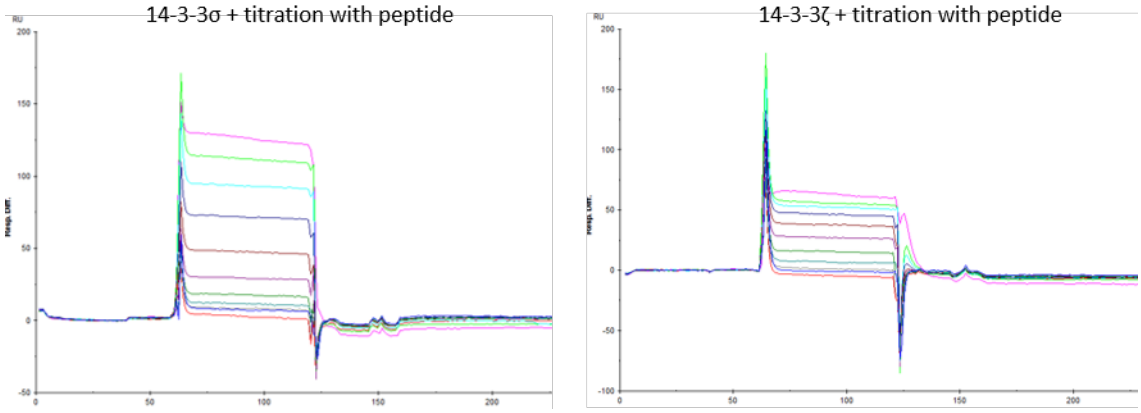

Figure SI-5. SPR sensograms for c-Abl peptide binding to h14-3-3σ and h14-3-3ζ. Various c-Abl peptide concentrations were passed over an immobilized h14-3-3 surface to a flow rate of 20 µL min^{-1}.

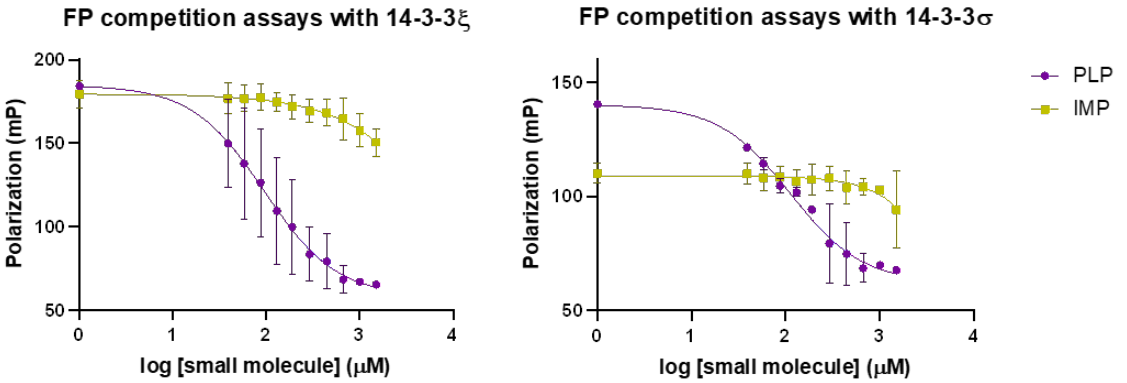

Figure SI-6. Dose-response curves determined for PLP and IMP during FP competition assays.

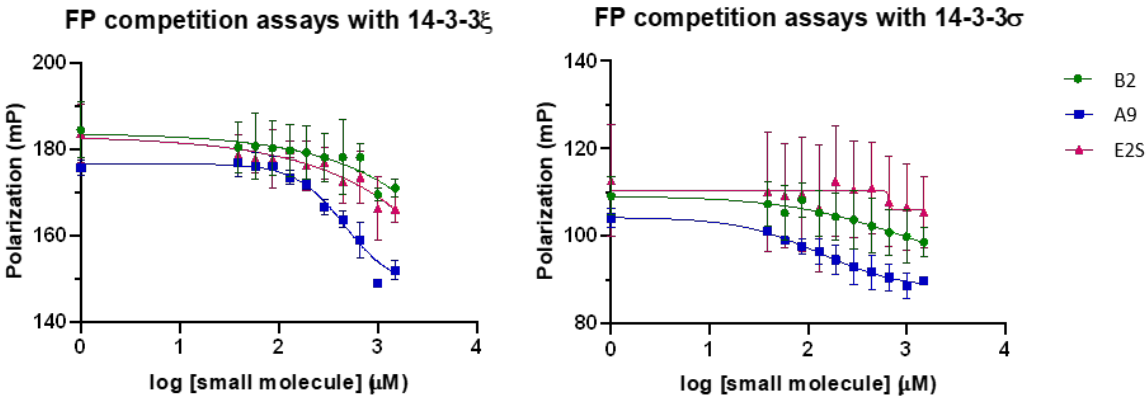

Figure SI-7. Dose-response curves determined for compounds B2, A9, and E25 during FP competition assays.

Table SI-1. Data collection and refinement statistics. Values for the outer shell are given in parentheses.

DATA COLLECTION STATISTICS

	h14-3-3σ	**h14-3-3σ**	
		PLP	**IMP**
PDB ID codes	**6TLG**	**6TM7**	**6TLF**
Diffraction source	ID30-B (ESRF)	I04-1 (DLS)	I04-1 (DLS)
Wavelength (Å)	0.9763	0.9159	0.9159
Temperature (K)	100	100	100
Detector	PILATUS3 6M	PILATUS 6M-F	PILATUS 6M-F
Crystal-detector distance (mm)	411.2	475.8	454.7
Rotation range per image (°)	0.1	0.3	0.3
Exposure time per image (s)	0.02	0.5	0.5
Space group	$I2_12_12_1$	$P2_12_12_1$	$I2_12_12_1$
No. of molecules/ASU	1	2	1
a, *b*, *c* (Å)	63.44 103.39 157.53	63.27 102.66 157.30	63.29 100.90 157.02
Resolution range (Å)	86.44-2.40 (2.53-2.40)	85.97-3.00 (3.16-3.00)	84.88-2.90 (3.06-2.90)
Total no. of reflections	78328 (12101)	105615 (14308)	59927 (8346)
No. of unique reflections	19842 (2964)	21085 (3016)	11508 (1638)
Completeness (%)	96.6 (98.9)	99.4 (99.5)	100.0 (100.0)
Redundancy	3.9 (4.1)	5.0 (4.7)	5.2 (5.1)
$\langle I/\sigma(I)\rangle$	5.6 (2.2)	7.8 (2.1)	10.1 (2.1)
R_{meas}	0.122 (0.461)	0.220 (0.677)	0.116 (1.033)
Overall *B* factor from Wilson plot (Å^2)	39.6	46.4	63.3

REFINEMENTS STATISTICS

	h14-3-3σ	**h14-3-3σ**	
		PLP	**IMP**
Resolution range (Å)	58.92-2.40 (2.46-2.40)	78.65-3.00 (3.08-3.00)	78.63-2.90 (2.98-2.90)
No. of reflections, working set	18747 (1428)	18250 (1449)	10921 (788)
No. of reflections, test set	1023 (67)	968 (66)	586 (35)
Final R_{cryst}	21.19 (35.1)	21.35 (35.1)	20.88 (32.9)
Final R_{free}	25.37 (30.8)	26.87 (46.6)	24.57 (30.7)
No. of non-H atoms			
Protein	1756	3397	1686
Sulfate anion	30	10	5
Ligand (PLP or IMP)	-	16	23
Others (di(hydroxyethyl)ether)	7 73	55	22
Water	1866	3478	1736
Total			
R.m.s. deviations			
Bonds (Å)	0.007	0.008	0.012
Angles (°)	1.688	1.961	1.990
Average *B* factors (Å^2)	56.93	53.24	79.07
Estimate error on coordinates based on R value (Å)	0.214	0.603	0.403
Ramachandran plot			
Most favored (%)	96.0	88.5	84.9
Allowed (%)	4.0	11.5	15.1
RSCC (PLP or IMP)		0.90	0.85

Table SI-2. Chemical structures of the compounds belonging to series A-E.

Series A: PLP derivatives				
A1	A2	A3	A4	A5
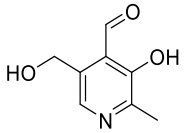	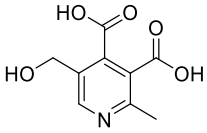	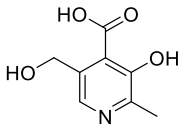	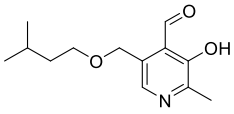	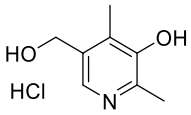
A6	A7	A8	A9	A10
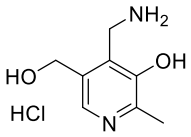	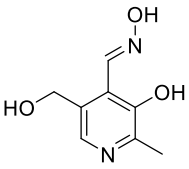	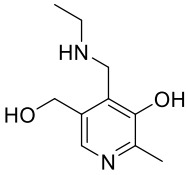	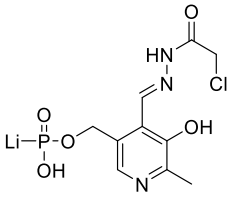	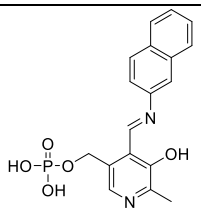
A11	A12	A13	A14	A15
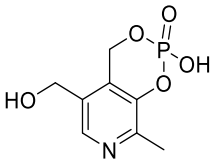	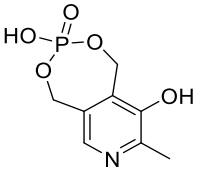	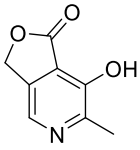	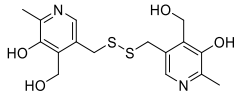	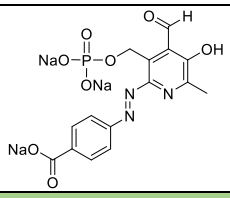
Series B: IMP derivatives				
B1	B2	B3	B4	
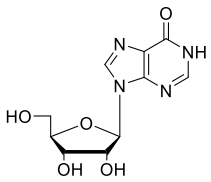	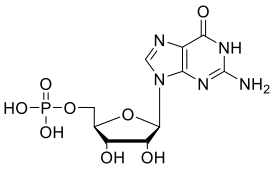	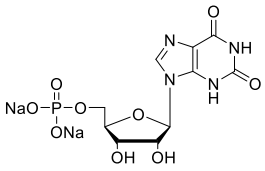	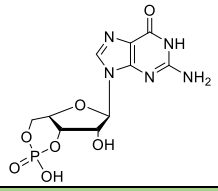	
Series C: Phosphonate and phospho-derivates (phosphorodiamidate)				
C1S	C2	C3	C4	C5
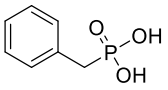	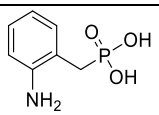	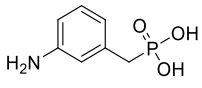	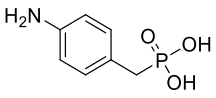	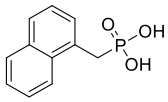
C5	C6S	C7S	C8	C9
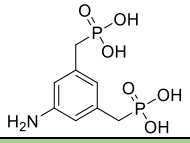	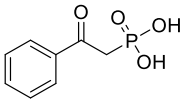	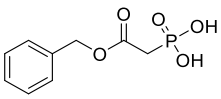	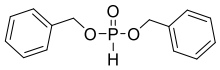	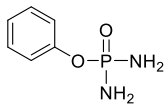
Series D: A13 derivatives				
D1	D2	D3	D4	
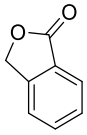	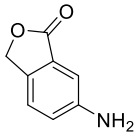	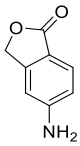	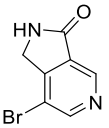	
Series E: PLP derivatives				
E1	E2S	E3	E4	E5
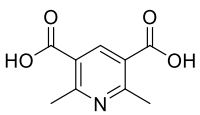	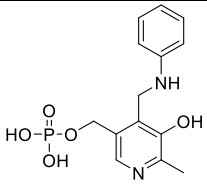	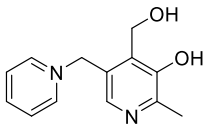	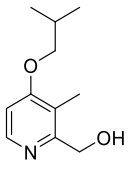	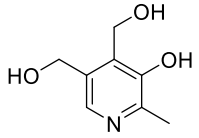

ABBREVIATION LIST

IMP, inosine monophosphate; PLP, pyridoxal phosphate; Fmoc, fluorenylmethyloxycarbonyl protecting group; Bn, benzyl group; TFA, trifluoroacetic acid; TIS, triisopropylsilane; HPLC, high performance liquid chromatography; MS, mass spectrometry; DMSO, dimethyl sulfoxide; NTA chip, nitrilotriacetic acid chip; RU, resonance units; NMR, nuclear magnetic resonance; FP, fluorescence polarimetry; SPR, surface plasmon resonance; DCM, dichloromethane; DCE, dichloroethane; MeOH, methanol.

References:

(1) Nihira, K.; Taira, N.; Miki, Y.; Yoshida, K. TTK/Mps1 Controls Nuclear Targeting of c-Abl by 14-3-3-Coupled Phosphorylation in Response to Oxidative Stress. *Oncogene* **2008**, *27*, 7285–7295.

(2) Stevers, L. M.; Lam, C. V; Leysen, S. F. R.; Meijer, F. A.; van Scheppingen, D. S.; de Vries, R. M. J. M.; Carlile, G. W.; Milroy, L. G.; Thomas, D. Y.; Brunsveld, L.; et al. Characterization and Small-Molecule Stabilization of the Multisite Tandem Binding between 14-3-3 and the R Domain of CFTR. *Proc. Natl. Acad. Sci. U. S. A.* **2016**, *113*, E1152-E1161.

(3) Iralde-Lorente, L.; Cau, Y.; Clementi, L.; Franci, L.; Tassone, G.; Valensin, D.; Mori, M.; Angelucci, A.; Chiariello, M.; Botta, M. Chemically Stable Inhibitors of 14-3-3 Protein–Protein Interactions Derived from BV02. *J. Enzyme Inhib. Med. Chem.* **2019**, *34*, 657–664.

(4) Kapust, R. B.; Tözsér, J.; Fox, J. D.; Anderson, D. E.; Cherry, S.; Copeland, T. D.; Waugh, D. S. Tobacco Etch Virus Protease: Mechanism of Autolysis and Rational Design of Stable Mutants with Wild-Type Catalytic Proficiency. *Protein Eng. Des. Sel.* **2001**, *14*, 993–1000.

(5) Benzinger, A.; Popowicz, G. M.; Joy, J. K.; Majumdar, S.; Holak, T. A.; Hermeking, H. The Crystal Structure of the Non-Liganded 14-3-3σ Protein: Insights into Determinants of Isoform Specific Ligand Binding and Dimerization. *Cell Res.* **2005**, *15*, 219–227.

(6) Benvenuti, M.; Mangani, S. Crystallization of Soluble Proteins in Vapor Diffusion for X-Ray Crystallography. *Nat. Protoc.* **2007**, *2*, 1633–1651.

(7) Leslie, A. G. W.; IUCr. The Integration of Macromolecular Diffraction Data. *Acta Crystallogr. D Biol. Crystallogr.* **2006**, *62*, 48–57.

(8) Kabsch, W. *XDS*. *Acta Crystallogr. D Biol. Crystallogr.* **2010**, *66*, 125–132.

(9) Evans, P. Scaling and Assessment of Data Quality. *Acta Crystallogr. D Biol. Crystallogr.* **2006**, *62*, 72–82.

(10) Evans, P. R. An Introduction to Data Reduction: Space-Group Determination, Scaling and Intensity Statistics. *Acta Crystallogr. D Biol. Crystallogr.* **2011**, *67*, 282–292.

(11) Winn, M. D.; Ballard, C. C.; Cowtan, K. D.; Dodson, E. J.; Emsley, P.; Evans, P. R.; Keegan, R. M.; Krissinel, E. B.; Leslie, A. G. W.; McCoy, A.; et al. Overview of the CCP4 Suite and Current Developments. *Acta Crystallogr. D Biol. Crystallogr.* **2011**, *67*, 235–242.

(12) Vagin, A.; Teplyakov, A.; IUCr. Molecular Replacement with *MOLREP*. *Acta Crystallogr. D Biol. Crystallogr.* **2010**, *66*, 22–25.

(13) Murshudov, G. N.; Skubák, P.; Lebedev, A. A.; Pannu, N. S.; Steiner, R. A.; Nicholls, R. A.; Winn, M. D.; Long, F.; Vagin, A. A.; IUCr. *REFMAC* 5 for the Refinement of Macromolecular Crystal Structures. *Acta Crystallogr. D Biol. Crystallogr.* **2011**, *67*, 355–367.

(14) Matthews BW. Solvent content of protein crystals. *J Mol Biol.* **1968**, *33*, 491-497.

(15) Emsley, P.; Lohkamp, B.; Scott, W. G.; Cowtan, K. Features and Development of Coot. *Acta Crystallogr. D Biol. Crystallogr.* **2010**, *66*, 486–501.

(16) Laskowski, R. A.; MacArthur, M. W.; Moss, D. S.; Thornton, J. M.; IUCr. PROCHECK: A Program to Check the Stereochemical Quality of Protein Structures. *J. Appl. Crystallogr.* **1993**, *26*, 283–291.
(17) PyMOL | Schrödinger https://www.schrodinger.com/pymol
(18) Yung-Chi, C.; Prusoff, W. H. Relationship between the Inhibition Constant (KI) and the Concentration of Inhibitor Which Causes 50 per Cent Inhibition (I50) of an Enzymatic Reaction. *Biochem. Pharmacol.* **1973**, *22*, 3099–3108.